Finite Element Modelling of the Vibration of a Power Transformer

Yuxing Wang, Jie Pan and Ming Jin

The University of Western Australia, Crawley WA 6009, Australia

ABSTRACT

As one of the most expensive and critical parts of power systems, power transformer maintenance and condition monitoring attracts increasing attention. Vibration analysis, which can be made either by experimental measurements or from predictions, is a promising technique in the health diagnosis of the power transformers. This paper presents the study of vibration characteristics of a power transformer mainly based on FEM. An improved FEM simulation scheme including electromagnetic simulation and the structural dynamic response analysis is presented. The complex vibration behaviour of the transformer is studied. Furthermore, this vibration model combining with vibration measurement may provide a potential method of diagnosing the failure modes of power transformer, such as looseness of clamp pressure and winding deformation. The reliability of the model scheme is verified by experimental measurement of a 10kVA power transformer.

1. INTRODUCTION

The working status of a power transformer directly relates to the electrical safety. Health diagnostic methods based on theoretic modelling and experimental conclusions have been studied for decades. The temperatures, cooling oil components, electrical and mechanical properties of parts of interest are all involved in various monitoring or diagnosing systems. However, the leading techniques can be summarized as frequency response analysis (FRA), leakage reactance measurement (LRM), and vibration analysis [1-3]. From the statistical analysis of some typical transformer failures, a common consensus about transformer failure modes is reached. The eventual damage of the failed power transformers in catastrophic incidents is winding deformation, fracture or melting in different ways. At least 12 to 15% of transformer failures are caused by winding deformations provoked by the high electro-dynamic forces appearing during short circuits [4]. As a result, the transformer vibration will change due to these deformations. Reflected to the transformer structure, the dynamic response is of great importance and a comprehensive understanding of dynamic response of such structures will provide further transformer health diagnosis.

Due to the complexity of transformer structure and its working conditions, analytical modelling meets insurmountable barriers. Some research can be found in analytical modelling of transformer windings [5], but it is far from explaining the transformer vibration features. As a boost to transformer condition monitoring, transformer models which come from experimental data analysis provide valuable understandings of the transformer vibration. However, the models themselves can only provide limited information as they mainly focus on a few vibration properties in certain frequencies.

FEM is employed as an alternative tool both solving electromagnetic and structure dynamic problems. Aimed at investigating the dynamic response of the power transformer under different loadings and boundary conditions, this paper proposes a FEM simulation scheme for the transformer modelling. Furthermore, an appropriate vibration monitoring method detecting transformer internal geometry deformations can be established. The study mainly focuses on vibration response at low frequency without cooling oil. The winding deformation and looseness of clamping pressure based on this model will be discussed in the near future.

2. MODELLING OF THE POWER TRANSFORMER

The transformer modelling scheme can be divided into two parts: detailed electro-magnetic force calculation and transformer structure dynamic analysis.

2.1 TEST POWER TRANSFORMER PROPERTIES

Figure1 shows the experimental transformer model. It comprises a 10kVA single phase 415/240V step-down disk-type transformer. Its nominal current in the primary winding is 20A with 240 turns and the secondary is 35A with 140 turns.

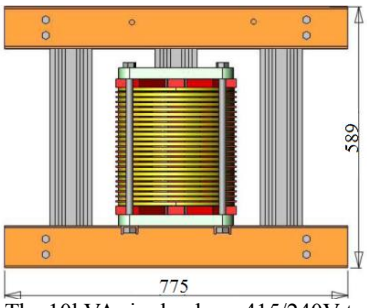

Figure 1. The 10kVA single phase 415/240V transformer

The transformer assembly is composed of multiple material and their properties are listed in table 1.

Table 1. Material property data

Part	*Material*	*Density (kg/m^3)*	*Young's Modulus (GPa)*	*Poisson ratio*
Winding	Copper	8900	115	0.35
Core	Silicon steel	7650	195	0.25
Brace	Steel	7850	210	0.3
Insulation block	Phenolic	820	20.72	0.4
Clamping plate	PBT	900	7.69	0.48

2.2 TRANSFORMER STRUCTURE DYNAMIC ANALYSIS

In this part, the dynamic response of the power transformer is simulated using FEM. In light of the experimental validation using an impact hammer test, only a unit force is applied on the first winding disc. As long as the transformer assembly is supported over steel brackets in practice, four springs is padded below the bottom core with four MPC (Multipoint Constraint Element) elements connected to simulate this boundary condition. The MPC element can be seen at the bottom of the transformer braces, as yellow and red line clusters, see Figure 2. The pre-tension force in each bolt clamping the winding assembly is 2250N and core assembly is 1500N.

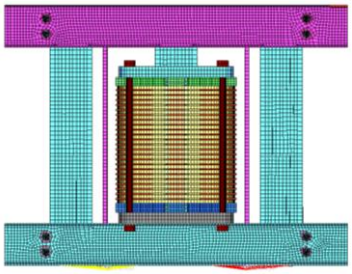

Figure 2. Transformer model for structure analysis

Before processing the structure dynamic analysis, a static step considering gravity and bolt loadings is employed to simulate the stress status under these conditions. Figure 3 gives a contour plot of the maximum principal stress. Although the pre-tension force applied in the central four bolts is 750N larger than those of other bolts tightening core assembly, the principal stresses at the brace surfaces are higher.

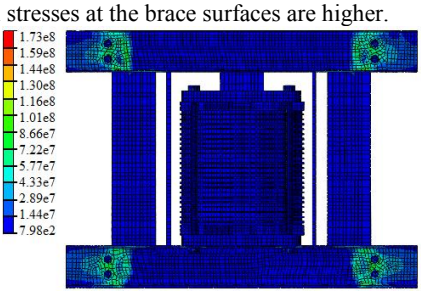

Figure 3. Stress distribution under clamping force (Pa)

Based on the transformer model and presetting steps, modal analysis and frequency response analysis can be proceeded to study its dynamic properties.

3. EXPERIMENTAL VERIFICATIONS

3.1 MODAL TEST

The verification of the transformer modal described above has been performed by a modal test. A B&K impact hammer (8206) was used to provide external force on the windings or core. Two B&K ICP accelerometers (4396) were used to measure the vibration at various locations of the transformer. A B&K Pulse (3560) multiple-input-system was used for data acquisition and frequency response functions. Figure 4 shows the schematic diagram for transformer modal test.

These 48 testing points acceleration were measured, uniformly distributed along transformer core (40 points) and winding assembly (8 points). Both top and lateral faces of core are measured with 10 points respectively. The top testing points are numbered from face to right from 1 to 10 and are measure the vibration in the Z direction. The testing points on the lateral face are numbered from left to right 11 to 20, which are arranged for vibration measurement in the X direction. The bottom core follows the same order as well with numbers 21-30, 31-40 respectively. The test transformer was supported on two blocks at the bottom of left and right core identical with the FEA model. All the illustrations showing in this paper are in the same coordinate represented in Figure 4.

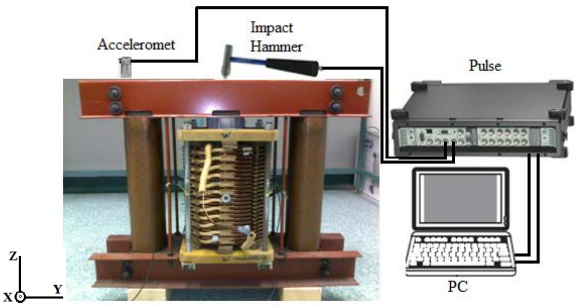

Figure 4. Transformer model for structure analysis

3.2 RESULTS ANALYSIS AND MODAL COMPARISON

In the modal test, the frequency response function (FRF) is obtained at each testing point. For such a complex structure, it is impossible to reflect all the vibration information at one testing point. Therefore, we averaged the kinetic energy in core and winding separately, see Figure 5. The dashed line represents the simulated FRF and solid line test FRF. The resonance peaks at 52 Hz and 240Hz is quite clear both in core and winding FRF plots. Further investigation from the FEA results shows that transformer vibrates in phase at 52Hz and winding rotates in-plane at 240Hz, see Figure 6. The dominant vibration in the windings is detected at testing points in the core because of the coupling among each part in this vibration system. For example, the second peak at 131.5Hz of test FRF in Figure 5(b) can be found in Figure 5(a) around 110Hz as the coupled result. Fortunately, this phenomenon is reflected in the simulated result which can be found at 140Hz as well, see Figure 5(a). Due to the heavy structure damping, the resonance peaks at certain frequency are not clear in higher frequency range.

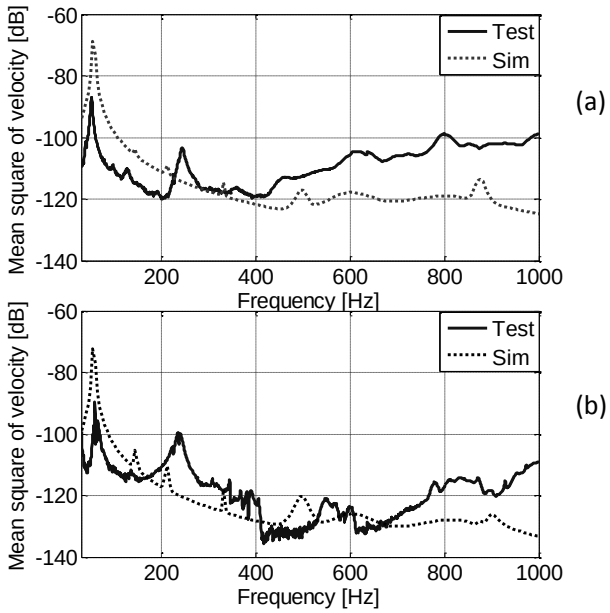

Figure5. FRF of the transformer: (a) core (b) winding

For such a complex dynamic system, the vibration in different parts may affect each other and coupled together. This increases the complexity of the modes. From the comparisons of tested and simulated FRF in both the core and the winding, some agreement can be found in low frequency range.

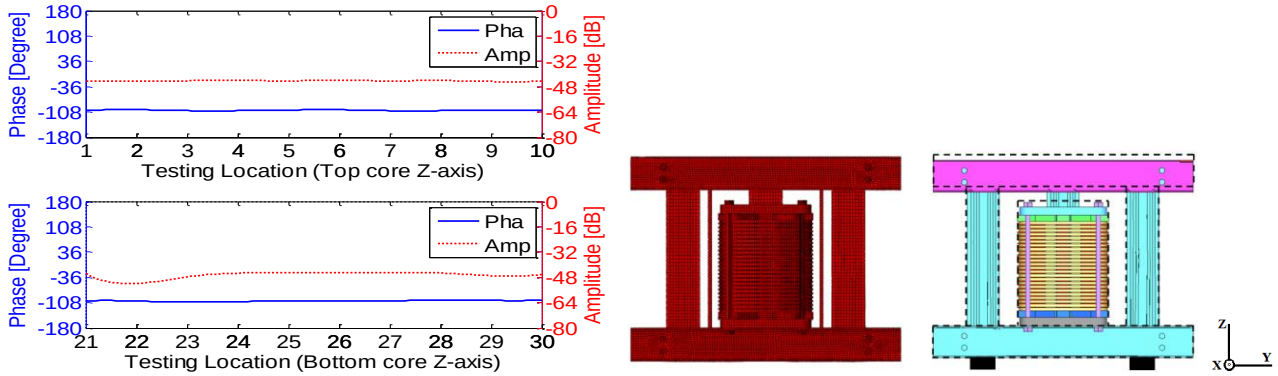

(a) 1st mode shape at 56.4Hz (Sim)/52.0Hz (Exp)

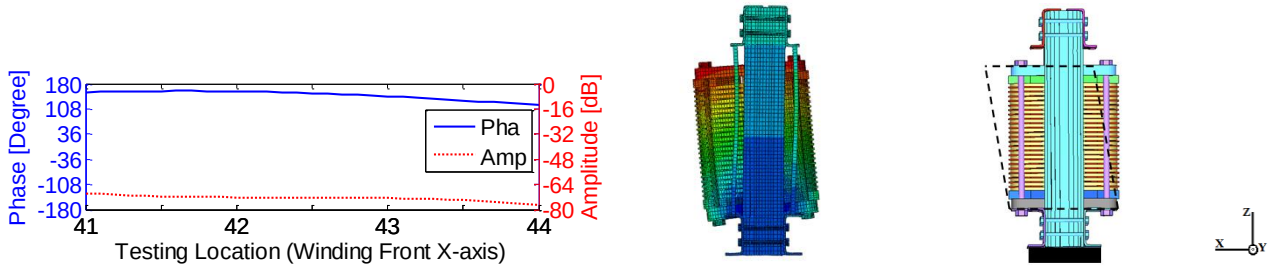

(b) 2nd mode shape at 145.0Hz (Sim)/131.5Hz (Exp)

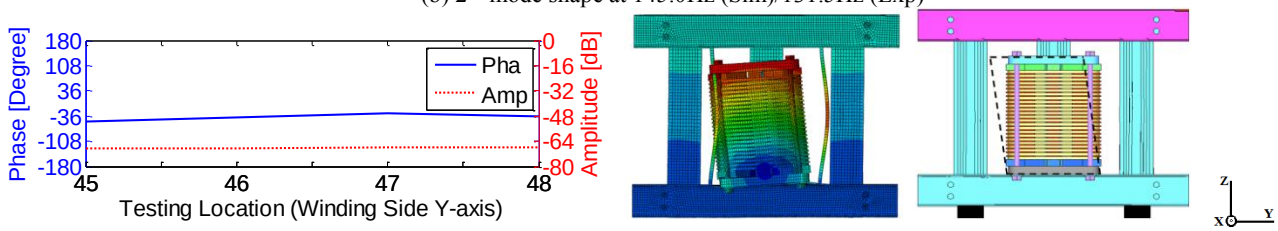

(c) 3rd mode shape at 210.9Hz (Sim)/240.0Hz (Exp)

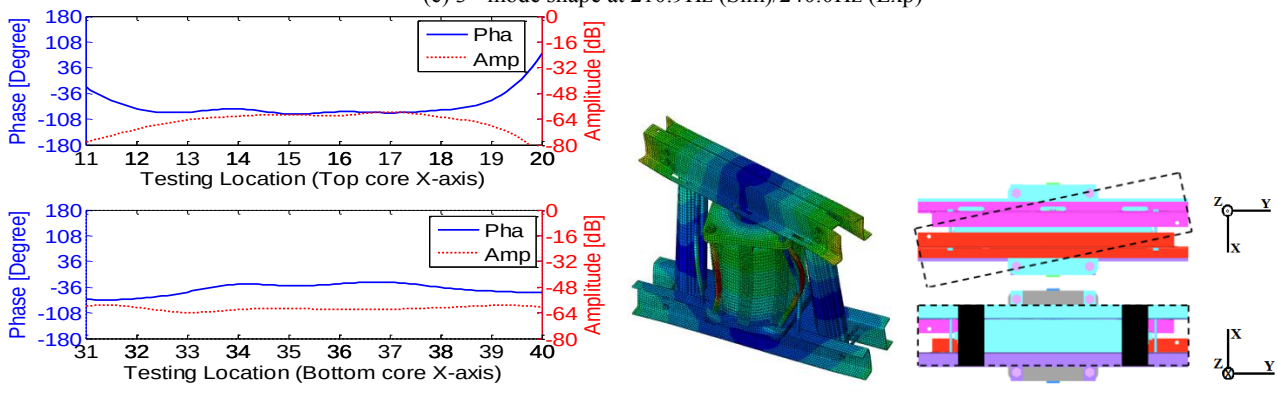

(d) 4th mode shape at 331.5Hz (Sim)/353.5Hz (Exp)

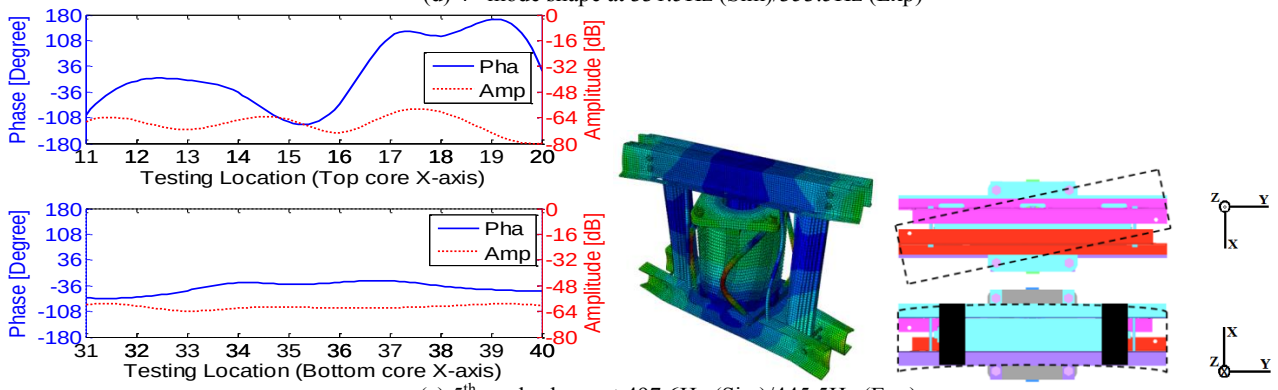

(e) 5th mode shape at 497.6Hz (Sim)/445.5Hz (Exp)

Figure 6. Mode shapes of the power transformer

To verify the FEM model and explain the vibration features of the power transformer, the mode shapes were summarized in

Figure 6.

The 1st mode in Figure 6(a) is the entire structure moving in phase, and simulated results shows good agreement both in mode shape and frequency deviation (8.46%). The 2nd mode in Figure 6(b) is the winding rotating out-of-plane and the 3rd mode rotation in-plane, and in both modes the winding moves in phase. The reason explaining the resonance for these two modes lies in the support location. The in-plane support length is longer than that of out-of-plane direction. Therefore, the resonance frequency for the in-plane vibration is higher due to the addition stiffness. That is, although the transformer may be considered as an axial symmetric structure in some cases for simplification, the results provided may only be used in narrow field.

Basically, the 4th and 5th modes are all related to the core distortion, but show total differences. The core window distorts in opposite direction with the winding assembly at the 4th mode, while distorts in the same direction at the 5th mode. The experimental results at the top core shows obvious distortion in both modes with the two ends vibrate in anti phase. At the same time, experimental modes in both bottom core reflects no such distortion features, but also not vibrate in phase. From the simulated results, there is a slight bending observed in both 4th and 5th modes at bottom core. The impact energy is not enough to fully excite the high frequency mode in such a heavy damped system.

4. TRANSFORMER VIBRATION BY ELECTROMAGNETIC FORCES

4.1 ELECTRO-MAGNETIC FORCE CALCULATION

In practice transformer winding vibration is generated by the currents in the HV and LV windings and the leakage magnetic flux intensity through the windings. Therefore, the prediction of EM force plays a fundamental role in transformer modelling. The electromagnetic field inside the transformer is governed by the following differential equation [6]:

$$\nabla\times\left(\frac{1}{\mu}\nabla\times A\right)=J_e-\gamma\frac{\partial A}{\partial t}-\gamma\nabla V \quad , \qquad (1)$$

where $\mathbf{J_e}$ represents the source current density, **A** the magnetic vector potential (MVP), μ the permeability, V the scalar electric potential and γ the electrical conductivity. The second term of the right-hand side of equation (1) represents the induced eddy current density in an electrically conductive body at rest, which is placed in a time-varying magnetic field. The third term of equation (1) expresses the current density due to the potential difference in a conductor [7].

FEM is used to calculate the magnetic vector potential and eventually obtain the EM force in transformer windings. A detailed 3D transformer model is presented in Figure 7.

In this analysis, we assume:

(1) Currents in HV and LV windings are uniformly distributed and flow in opposite directions;

(2) Current densities in the HV and LV windings are 7.48×10^5 A/mm^2 and 5.0×10^5 A/mm^2 respectively corresponding to 1A current input in the primary end.

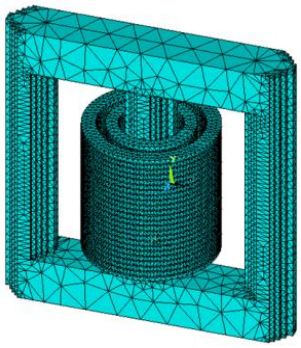

Figure 7. Transformer model for electromagnetic simulation

It should be emphasized that the entire magnetic circuit is retained. In addition, the 3D model for electro-magnetic simulation is the same as the following structure analysis without simplification.

Using the electromagnetic transformer model (Figure 7), the leakage magnetic flux density is calculated using FEA and shown in Figure 8.

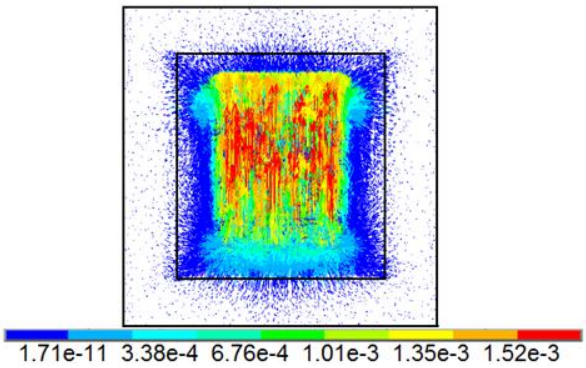

(a) 3D Leakage flux density

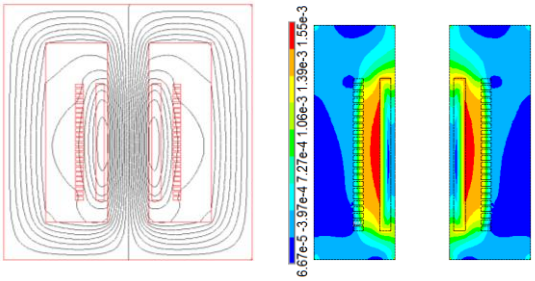

(b) 2D flux line (c) 2D leakage flux density

Figure 8. Leakage flux density of the power transformer (T)

Figure 8(a) shows a vector plot of the transformer leakage flux within core areas. The EM force calculation needed in the following vibration prediction comes from this magnetic field.

With regard to a clear demonstration of such a leakage flux density, 2D simulation under the same boundary condition was employed. Figure 8 represents the longitudinal cross section of the transformer and the leakage flux is produced by the equal ampere-turns.

From the comparison of leakage flux density between 2D and 3D simulation, we can see a good agreement both in the distribution and the magnitude with 1.55×10^{-3}T and 1.52×10^{-3}T separately. The magnetic field between HV and LV windings is strengthened as current flows in converse directions at the same time weakened within the LV winding area and outside area of the HV winding. For a specific winding disc, e.g. the middle disc of HV winding, leakage flux in the axial direction at the inner turns is larger than that of

outer turns. The same conclusion is drawn by many researches [8-9]. Figure 8 represents a rapid attenuation of flux intensity with the distance. A clear symmetric in the middle section can be seen both from 2D flux line distribution and contour plot of leakage flux. From the 2D flux distribution, it can also be seen that leakage flux is much smaller than main flux.

Based on the simulated leakage flux, the EM force of the distributed ampere-turns was calculated and summarized within each winding disc, Figure 9.

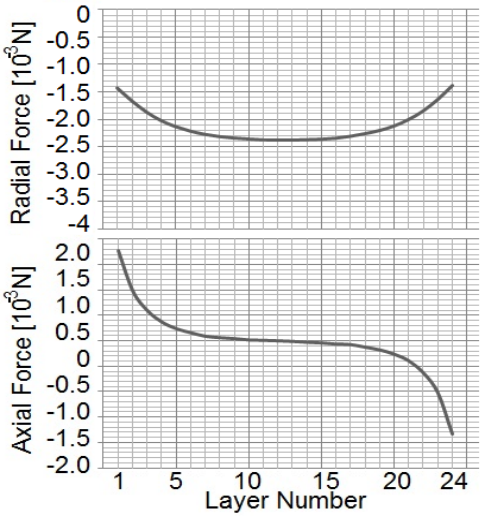

(a) HV winding EMF

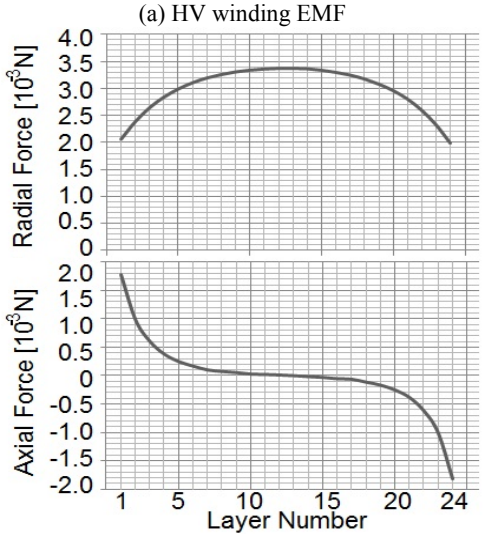

(b) LV winding EMF (N)

Figure 9. EMF of transformer windings in axial and radial direction

The EM force can be decomposed into radial and axial components, which are produced by corresponding parts of leakage flux. Figure 9 represents the EM force distribution of each winding disc along axial and radial directions and shows a good agreement with analytical explanations in [8]. From the force distribution in axial direction in both HV and LV winding, the same trend can be found that axial force tends to compress these two winding stacks. (Layer No.1 is the bottom winding disk and No.24 is the top one.).When it comes to the radial EM force, EM force shows compression tendency for the LV winding and expansion tendency for the HV winding. The maximum axial EM force occurs at top and bottom layers while the maximum radial one at the middle winding disc. The radial EM force is bigger than axial EM force in this transformer model. Although it may not be applicable to every type of power transformer, it should be noted that each component of EM force in transformer winding cannot be neglected. Based on this conclusion, a pair of top and middle winding discs is specially discussed.

Figure 10 illustrates the leakage flux and EM force in transformer winding in axial and radial directions. The positive force in radial distribution represents winding elongation along radius direction and negative value means compression in outward direction. In axial direction, positive and negative represents EM force in positive and negative Z-axis in the general coordinate. Symmetry about cross section in YZ plane can be seen both in the leakage flux and EM force while the symmetric features of EM force has small flaws.

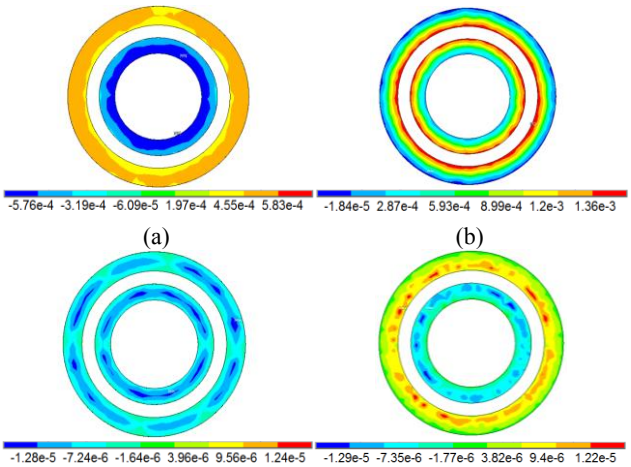

Figure 10. FEM response of flux density (T) and EM force (N) in HV and LV winding discs: (a) Flux density of top winding disc in radial direction (b) Flux density of middle winding disc in axial direction (c) EM force of top winding disc in axial direction (d) EM force of middle disc in radial direction

4.2 TRANSFORMER VIBRATION

Vibrations in transformer are generated by two main sources: magneto striction of the core [9] and winding vibration due to EM force. In this paper, we only focus on the winding vibration. Core vibration will be taken into account in the future works. EM force is proportional to the current squared; therefore, the fundamental vibration at 100Hz and its harmonics show vital importance since current is practically 50Hz in Australia.

The calculation of forced vibration under distribution EM force is implemented using the FEA transformer model which has been verified in previous parts. Here, we assume the distribution of EM force in each winding disc is uniform, see Figure 11. The enlarged part shows a distribution of calculated EM force in the FEA model (dark arrows). The pre-tension force and gravity component are also considered during the vibration simulation. Figure 11 represents the vibration features at 100Hz by means of velocity. The overall vibration of this transformer is dominated by the 1st mode and each part vibrating in phase as one entirety. From Figure 11 we also can see the asymmetric distribution of vibration velocity, as the vibration at 100 Hz is a composite results by mode superposition.

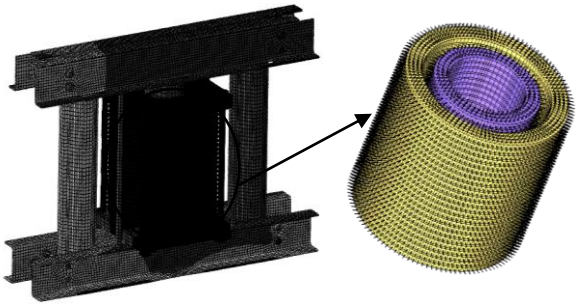

Figure 11. Contour plot of transformer vibration feature (velocity) at 100 Hz

With regard to the winding itself, the vibration pattern under such a distributed force also shows the same interesting phenomena. In the transformer modal analysis, the vibration of winding assembly at low frequency range is dominated by rotation around the supporting bracket. Figures 12 and 13 show the winding vibration at HV outer surface which are expressed along circumferential direction from 0 to 180 degree at different frequencies. Since the LV winding shows the same tendency, only outer winding (HV) is discussed. Vibration properties are firstly discussed at the 2nd and 3rd natural frequencies in which winding rotation can be observed. In Figure 12, the forced vibration at 145Hz and 240Hz both in axial and radial direction are represented, from which we can see the rotation clearly out-of-plane (145 Hz) and in-plane (240Hz) as mentioned in modal analysis. All these contour plots are drawn as the transformer placed in Figure 6(b).

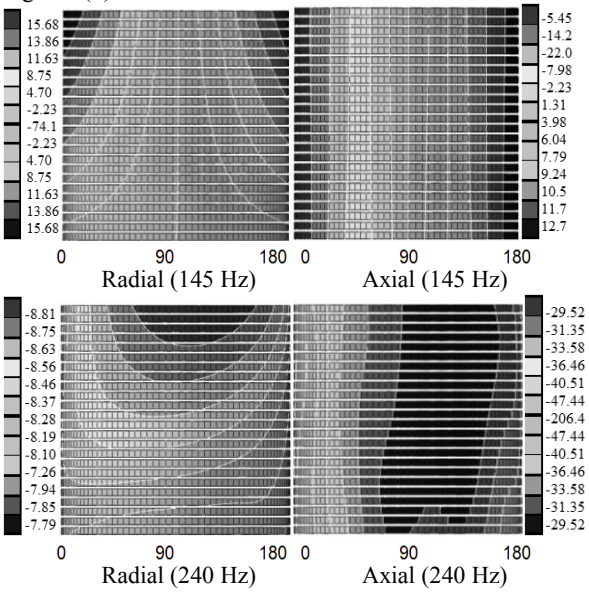

Figure 12. Outer surface vibration of the HV winding (velocity) at 145Hz, 240Hz

In practice, winding vibration at 100Hz and its harmonics contribute to the dominant parts of transformer vibration caused by current and leakage flux. As to this power transformer, the forced vibrations of the power transformer at 100Hz and 200Hz are superpositions of the nearby mode shapes, which rotate out-of-plane and in-plane around the support bracket, see Figure 13.

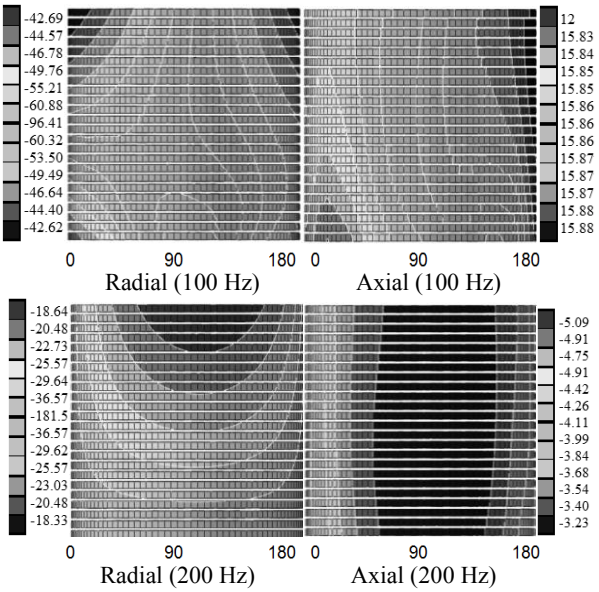

Figure 13. Contour plot of winding vibration (velocity) at 100Hz, 200Hz

Due to the space limitations, only a 200Hz vibration is presented in this paper as a representative example, see Figure 13. As expected, it is found obviously that the dominant vibration feature at 200Hz comes from 240Hz mode.

4. CONCLUSIONS

In this paper, an improved FEM simulation scheme including electromagnetic simulation and structure dynamic response analysis is presented and successfully applied to a power transformer. The deviation between experimental and simulated natural frequency is below 10%. In addition, the simulated mode shapes agree well with the experimental results.

The complex vibration behaviour of a power transformer is studied, especially in the HV winding. From the above analysis, a general understanding of power transformer vibration mechanism is established when the transformer is properly clamped. The transformer vibrates as one entity the low frequency range under the above boundary conditions. The forced vibrations of power transformer at 100Hz and 200Hz are superposed by the nearby modes which rotate out-of-plane and in-plane around support bracket.

The presented FEM model has been shown as a useful tool to investigate the dynamic response of the power transformer. The reliability of this model scheme is verified by experimental measurement of a 10kVA power transformer. It also provides a potential way of diagnosing the failure modes of power transformer, such as looseness of clamp pressure and winding deformation. Further work will investigate vibration variation resulting from these factors.

ACKNOWLEDGEMENTS

We thank Dr. Andrew Guzzomi for proof reading the manuscript and useful suggestions. Financial support to this project by CRC for Infrastructure Engineering Asset Management (CIEAM) is gratefully acknowledged.

REFERENCES

[1] J. A. Lapworth & T. J. Noonan, '*Mechanical condition assessment of power transformers using frequency response analysis*', Proceedings of the 1995 International client conference, 1995, Boston, MA, USA.

[2] A. Babare, F. Cannata, G. Caprio, S. Sacchetti, & G. Zafferrani, '*Ennel-diagnossis of on- and off-line large transformers*', Proc. Cigré Symp, , 1993, Berlin, Germany.

[3] B. García, J. C. Burgos, & A. Alonso, '*Transformer tank vibration modeling as a method of detecting winding deformations—Part I: Theoretical foundation*', IEEE Trans. Power Del., 2006, Vol. 21, No. 1. pp. 157-163.

[4] V. Sokolov & B. Vanin, '*Experience with detection and identification of winding buckling in power transformers*', Proc. 68th Annu. Int. Conf. 2001, Doble Clients.

[5] S. C. Ji, '*Failure Monitoring Investigation of Transformer Wingding and Core Characteristic*', PhD thesis, 2003, Xi An Jiao Tong University.

[6] P. S. Silvester & R. L. Ferrari, '*Finite Elements for Electrical Engineers*', 1996, Vol. 3, Cambridge: Cambridge University Press, London.

[7] M. Rausch, M. Kaltenbacher, H. Landes & R. Lerch, '*Combination of finite and boundary element methods in investigation and prediction of load-controlled noise of power transformers*', J. Sound & Vib., 2002, Vol. 250, No. 2. pp. 323-328.

[8] L. F. Blume, G. Camilli, A. Boyajian & V. M. Montsinger, '*Transformer Engineering*', 1946, The General Electronic Company, USA.

[9] R. M. Bozorth, '*Ferromagnetism*', 1993, IEEE Press, New York